

# Miniature surface-mountable Fabry–Perot pressure sensor constructed with a 45° angled fiber

H. Bae,<sup>1</sup> X. M. Zhang,<sup>2</sup> H. Liu,<sup>1</sup> and M. Yu<sup>1,\*</sup>

<sup>1</sup>Department of Mechanical Engineering, University of Maryland, College Park, Maryland 20742, USA

<sup>2</sup>Department of Applied Physics, Hong Kong Polytechnic University, Hung Hom, Kowloon, Hong Kong, China

\*Corresponding author: mmyu@umd.edu

Received February 17, 2010; revised April 17, 2010; accepted April 20, 2010;  
posted April 23, 2010 (Doc. ID 124310); published May 14, 2010

We present a surface-mountable miniature Fabry–Perot (FP) pressure sensor that utilizes the total internal reflection at a 45° angled fiber end face to steer the optical axis by 90°. By using the fiber as a waveguide, as well as a natural mask in photolithography, an FP cavity is constructed on the sidewall of the fiber. A polymer–metal composite diaphragm is employed as the pressure transducer. The sensor exhibits a good linearity over the pressure range of 1.9–14.2 psi, with a sensitivity of 0.009  $\mu\text{m}/\text{psi}$  and a hysteresis of 2.7%. This sensor is expected to impact many fronts that require reliable static pressure measurements of fluids. © 2010 Optical Society of America

OCIS codes: 060.2370, 120.2230, 230.3990.

Miniature fiber-optic pressure sensors have become attractive choices for pressure monitoring in a limited space owing to their advantages of small size, high sensitivity, immunity to electromagnetic interference, and convenience of light guiding/detection through optical fibers [1]. Such a sensor typically exploits an extrinsic Fabry–Perot (FP) interferometer formed directly on a fiber end face, as illustrated in Fig. 1(a), which consists of a cleaved optical fiber, a pressure sensing diaphragm, and a housing structure for holding the diaphragm. The fiber end facet and the reflective diaphragm effectively form an FP cavity for sensing the external pressure. As the FP cavity shares the optical axis with the optical fiber, this configuration is named as *coaxial configuration*. A variety of miniature coaxial FP sensors have been reported in literature [2–9], and they have been applied to many applications, including biomedical [6,8,9], aerodynamic [7], and other industrial applications [3] where a minimal intrusiveness is required.

However, for pressure measurements in fluids, a coaxial sensor that is positioned toward the flow can pick up both dynamic and static pressures, which is known as the total pressure [10]. In this case, the flow is stopped at the pressure-sensing diaphragm, resulting in an increase in the pressure reading from the sensor. To eliminate the dynamic pressure effect and to obtain only the static pressure, a coaxial sensor should be carefully positioned so that the axis of the FP cavity is perpendicular to the direction of the flow. To facilitate such positioning, mounting the coaxial sensor on a structure surface usually requires bending of the fiber and/or drilling a through-hole on the surface, which is inconvenient and sometimes even impractical. Therefore, when it is important to distinguish the static pressure from the surface flow, an alternative sensor design that renders easy sensor surface mounting is needed. Such surface-mountable sensors are especially desirable for pressure measurements in blood vessels [6,11] and on-blade pressure monitoring of turbomachineries [3,7] and rotorcrafts [12].

In this Letter, we report a surface-mountable miniature FP pressure sensor. The schematic of the sensor is shown in Fig. 1(b), and it consists of a fiber with a 45° angled end face, a sensing diaphragm, and a housing

structure formed on the sidewall of the fiber to hold the diaphragm. The key concept here is to steer the optical axis by 90° based on total internal reflection at the 45° angled fiber end face. In this configuration, the fiber sidewall serves as a partial mirror of the FP interferometer, and the reflective diaphragm that is parallel to the fiber-optical axis serves as the other mirror. Because the fiber axis is perpendicular to that of the FP cavity, this configuration is called a *cross-axial configuration*. One unique feature of the cross-axial sensor is that it can be directly mounted on a structure surface or embedded in a shallow channel to accurately measure the static pressures even in the presence of surface flows.

The detailed fabrication process of the cross-axial FP pressure sensor is shown in Fig. 2. First, preparation of the angled fiber samples is performed [Fig. 2(a)]. A batch (typically 20–50) of single-mode fibers (SMF28, Corning) are spliced and glued on a glass slide by using a wax (mounting wax 70, Electron Microscopy Sciences) for polishing purposes. The fibers are polished to form the 45° angled end face with a fiber polishing machine. Calibration of the polished angles is carried out by measuring the reflection from the polished fiber end face. The reflection reaches its maximum when a 45° end face is achieved. A thin layer of silver is then evaporated onto the angled fiber end face to further enhance the reflection.

Second, a photoresist layer is deposited and UV exposed; this serves as the housing structure. The polished fiber is dipped into a positive photoresist (AZ 4620, Shipley) to cover the fiber sidewall with a thin layer of photoresist. Soft baking is then carried out at 95 °C for 5 min.

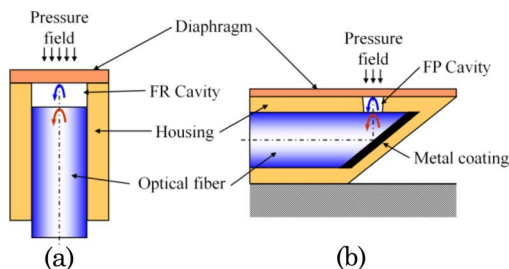


Fig. 1. (Color online) Configurations of miniature fiber-optic pressure sensors: (a) coaxial configuration and (b) cross-axial configuration.

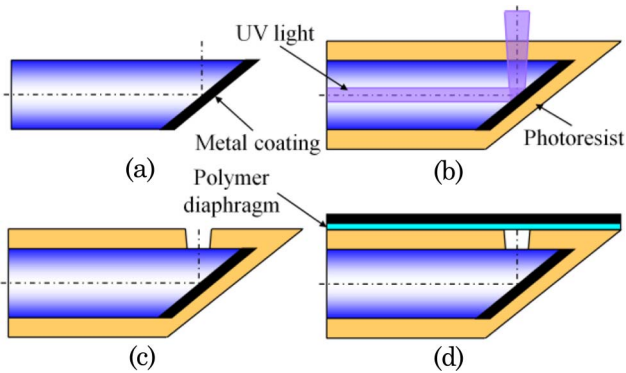


Fig. 2. (Color online) Fabrication process flow of the surface-mountable sensor: (a) polishing of the 45° angled fiber end face and deposition of the metal layer, (b) exposure of the photoresist housing with a fiber-coupled UV light, (c) development of the photoresist, and (d) covering of the polymer diaphragm and deposition of the reflective layer.

After each cycle of deposition and soft baking, a photoresist layer of 3–5  $\mu\text{m}$  will be formed on the fiber sidewall. As the cavity length of the FP interferometer is determined by the photoresist thickness, which is monitored by using an optical microscope (Olympus) and a digital camera (CFW-1308C, Scion Corporation), various cavity lengths can be obtained by performing different numbers of deposition/soft-baking cycles. After a desired thickness is obtained, light from a spot UV source (Blue-Wave 50S, DYMAX) is coupled into the fiber and reflected by the 45° angled end face to expose the photoresist along the light path; see Fig. 2(b).

Third, an air cavity serving as the FP cavity is formed in the photoresist. The exposed photoresist is developed by using a developer (AZ 440 K diluted 1:3) for 5 min to form the air cavity, as shown in Fig. 2(c). The sample is then hard baked at 100 °C for 5 min to enhance the stability of the remaining photoresist housing structure. The depth of the cavity is measured by using an optical profilometer (TMS 1200, Polytec) with a high resolution (0.195 nm). As the fiber waveguide is used as a photo mask, the cavity axis will be self-aligned to the optical path accurately without the need for any alignment systems or extra masks [13].

Finally, a polymer–metal composite diaphragm is prepared and covered on the housing. A drop of acrylic urethane UV polymer (OP-4-20641, DYMAX) is dispensed into deionized water in a petri dish (diameter of 100 mm). After spreading to a thin layer with a desired thickness, the polymer is half cured, and then lifted up and covered onto the housing structure. After full curing, a silver layer with a chromium adhesion layer is sputtered on the polymer film to enhance the reflectivity. Another optional protective polymer layer can be added later to isolate the metal layer from the external environment to avoid oxidization and corrosion. A detailed diaphragm preparation process can be found in [9]. The completed surface-mountable FP sensor is illustrated in Fig. 2(d). Both the thicknesses of the metal layer and the polymer layer can be tuned to meet the specific needs of various pressure-sensing applications.

In this work, a 1.3  $\mu\text{m}$  acrylic urethane film coated with 150 nm silver and 3 nm chromium was used as the dia-

phragm and a 13.8  $\mu\text{m}$  depth optical cavity was obtained on the fiber sidewall. The overall sensor diameter ( $\sim 150 \mu\text{m}$ ) is slightly larger than the fiber diameter (125  $\mu\text{m}$ ). The diaphragm diameter was measured to be around 18  $\mu\text{m}$ . The pressure sensitivity in terms of the diaphragm center deflection is predicted to be 0.0131  $\mu\text{m}/\text{psi}$  by using a finite element model. A scanning electron micrograph of the cavity before applying the diaphragm and a close-up of the composite diaphragm are shown in Fig. 3.

In the experiment, the fabricated FP sensor was connected to a white light interferometer system for interrogation. The system consists of a broadband light source (HL-2000 Tungsten Halogen Light Source, Ocean Optics), a 2 × 2 coupler (50/50), a spectrometer (USB4000, Ocean Optics), and a computer for data collection and signal processing [9]. The absolute cavity length  $L$  [see Fig. 1(b)] can be retrieved from the reflection spectrum of the spectrometer as  $L = \frac{\lambda_1 \lambda_2}{2\text{FSR}}$ , where  $\lambda_1$  and  $\lambda_2$  are any two adjacent peaks of the reflection spectrum and  $\text{FSR} = |\lambda_2 - \lambda_1|$  is the free spectral range [14]. The spectrometer has a spectral resolution of  $\sim 0.1 \text{ nm}$ , rendering a cavity length resolution of 3.5 nm. To reduce the error in finding the FSR, the curve fitting method was used [15]. The cavity length  $L$  was eventually calculated by averaging several FSRs obtained from the peaks with good visibility to further reduce the random errors.

Sensor calibration was conducted in a pressure chamber with a reference pressure sensor (LL-080-25A, Kulite Semiconductor Products). The pressure in the chamber was controlled by using a pressure regulator (R-68825-08, Marsh Bellofram) with a pressure regulation range of 1.9 to 60 psi. In the experiment, the pressure was first increased from 1.9 to 14.2 psi at room temperature, and then it was gradually decreased to atmospheric pressure. Figure 4 shows the calibration results, which exhibit a good linearity ( $R^2 = 0.99$ ). Based on the linear fitting of the experimental data, the pressure sensitivity of the sensor can be obtained to be around 0.009  $\mu\text{m}/\text{psi}$  in the pressure range of 1.9–14.2 psi, which compares well with the model predicted sensitivity (0.0131  $\mu\text{m}/\text{psi}$ ). Since the calibration curves obtained from increasing and decreasing pressures are almost overlapped, the hysteresis error of the sensor is not significant ( $\sim 2.7\%$ ). It is noted that the results exhibit a drift of the initial cavity length by 0.005  $\mu\text{m}$ , which is about 0.04% of the initial cavity length (13.8  $\mu\text{m}$ ). This small drift is found to be due to the ambient temperature variation (around a couple of degrees) observed during the

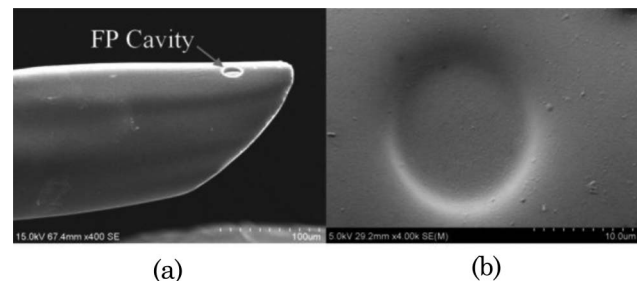


Fig. 3. Scanning electron micrographs of (a) optical cavity before covering the diaphragm and (b) the close-up of the composite diaphragm.

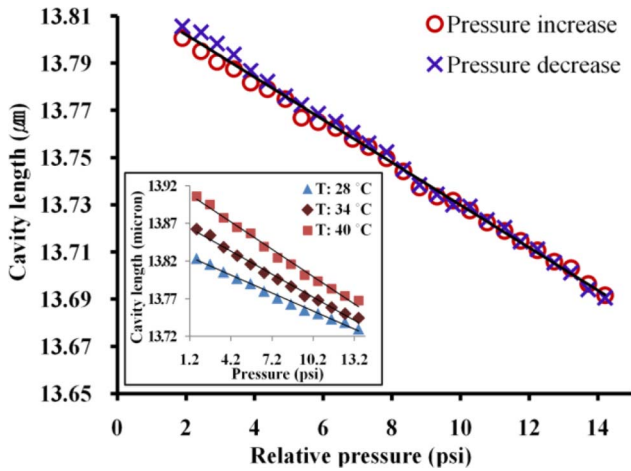


Fig. 4. (Color online) Sensor cavity length as a function of the external pressure.

experiment. Over a temperature range of  $T = 28\text{ }^{\circ}\text{C}$  to  $T = 40\text{ }^{\circ}\text{C}$ , the thermal effect on the sensor has been carefully studied. As shown in the inset of Fig. 4, both the initial cavity length and the pressure sensitivity show slight temperature-associated variations. In applications where temperature variations are of concern, an external temperature sensor or an additional FP cavity with a different initial cavity length can be included to provide temperature compensation.

To the best of the authors' knowledge, this is the first time that a miniature cross-axial FP pressure sensor has been developed. The cross-axial FP sensor possesses several unique features in terms of sensor design and fabrication as compared to the previously reported coaxial FP pressure sensors. First, the FP cavity is achieved on the fiber sidewall, rendering a surface-mountable sensor that can be simply attached to the structure surface for reliable static pressure measurements. Second, the fabrication follows simple, repeatable processes and safe procedures, and uses less expensive materials, without the need for a clean-room environment. Although photolithography is utilized for patterning the photoresist housing structure, the fabrication does not need any extra photo masks, as the FP optical cavity is self-aligned to the steered light path. This eliminates tedious optical alignments, which are usually quite challenging in the fabrication of a miniature fiber-optical sensor. Third, the multilayer design of the sensor diaphragm not only enhances the durability of the sensor but also allows for easy tuning of the sensor performance parameters (i.e., sensitivity and dynamic range).

In conclusion, a surface-mountable miniature FP pressure sensor is developed, which takes the advantage of the total internal reflection occurred at a  $45^{\circ}$  angled fiber end face to facilitate both cross-axial pressure sensing and photolithography. The experiment shows that the sensor has a linear response over a pressure range of 1.9–14.2 psi, with a sensitivity of  $0.009\text{ }\mu\text{m}/\text{psi}$ . It is expected that this sensor will benefit many areas that require miniature sensors for reliable static pressure measurements of fluids and gases.

We gratefully acknowledge support from the National Science Foundation (NSF) (CMMI0644914), the Center for Rotorcraft Innovations (W911W6-06-2-0002), the United States Army Research Office (USARO) Defense University Research Instrumentation Program (DURIP) (W911NF0710215), and the Maryland NanoCenter and its NispLab.

## References

1. Y. J. Rao, *Opt. Fiber Technol.* **12**, 227 (2006).
2. S. Watson, M. J. Gander, W. N. MacPherson, J. S. Barton, J. D. C. Jones, T. Klotzbuecher, T. Braune, J. Ott, and F. Schmitz, *Appl. Opt.* **45**, 5590 (2006).
3. W. N. MacPherson, J. M. Kilpatrick, J. S. Barton, and J. D. C. Jones, *Rev. Sci. Instrum.* **70**, 1868 (1999).
4. X. W. Wang, J. C. Xu, Y. Z. Zhu, K. L. Cooper, and A. Wang, *Opt. Lett.* **31**, 885 (2006).
5. D. C. Abeysinghe, S. Dasgupta, J. T. Boyd, and H. E. Jackson, *IEEE Photonics Technol. Lett.* **13**, 993 (2001).
6. K. Totsu, Y. Haga, and M. Esashi, *J. Micromech. Microeng.* **15**, 71 (2005).
7. M. J. Gander, W. N. MacPherson, J. S. Barton, R. L. Reuben, J. D. C. Jones, R. Stevens, K. S. Chana, S. J. Anderson, and T. V. Jones, *IEEE Sens. J.* **3**, 102 (2003).
8. E. S. Olson, *J. Acoust. Soc. Am.* **103**, 3445 (1998).
9. S. Nesson, M. Yu, X. M. Zhang, and A. H. Hsieh, *J. Biomed. Opt.* **13**, 044040 (2008).
10. V. L. Streeter and E. B. Wylie, *Fluid Mechanics*, 8th ed. (McGraw-Hill, 1985).
11. R. Melamud, A. A. Davenport, G. C. Hill, I. H. Chan, F. Declercq, P. G. Hartwell, and B. L. Pruitt, in *Proceedings of 18th International Conference on Microelectromechanical Systems* (2005), pp. 810–813.
12. Y. Liu, L. Alexander, G. Wang, P. Ashish, and M. Yu, *Proc. SPIE* **6770**, 67700Y (2007).
13. M.-S. Kim, K.-W. Jo, and J.-H. Lee, *Appl. Opt.* **44**, 3985 (2005).
14. K. T. V. Grattan and B. T. Meggitt, *Optical Fiber Sensor Technology* (Chapman & Hall, 1995).
15. B. Qi, G. R. Pickrell, J. Xu, P. Zhang, Y. Duan, W. Peng, Z. Huang, W. Huo, H. Xiao, R. G. May, and A. Wang, *Opt. Eng.* **42**, 3165 (2003).